Dynamic Diffusion Model for Tracing the Real-Time Potential Response of Polymeric Membrane Ion-Selective Electrodes

ARTICLE *in* ANALYTICAL CHEMISTRY · DECEMBER 2004

Impact Factor: 5.64 · DOI: 10.1021/ac049348t · Source: PubMed

3 AUTHORS:

Aleksandar Radu
Keele University
47 PUBLICATIONS **1,036** CITATIONS
SEE PROFILE

Amnon J Meir
Auburn University
36 PUBLICATIONS **377** CITATIONS
SEE PROFILE

Eric Bakker
University of Geneva
291 PUBLICATIONS **13,792** CITATIONS
SEE PROFILE

Anal. Chem. **2004,** *76,* 6402−6409

Dynamic Diffusion Model for Tracing the Real-Time Potential Response of Polymeric Membrane Ion-Selective Electrodes

Aleksandar Radu,[†] Amnon J. Meir,*[,‡] and Eric Bakker*[,†]

Departments of Chemistry and Mathematics, Auburn University, Auburn, Alabama 36849

A numerical solution for the prediction of the time-dependent potential response of a polymeric-based ion-selective electrode (ISE) is presented. The model addresses short- and middle-term potential drifts that are dependent on changes in concentration gradients in the aqueous sample and organic membrane phase. This work has important implications for the understanding of the real-time response behavior of potentiometric sensors with low detection limits and with nonclassical super-Nernstian response slopes. As a model system, the initial exposure of membranes containing the well-examined silver ionophore *O,O″*-bis[2-(methylthio)ethyl]-*tert*-butylcalix[4]arene was monitored, and the large observed potential drifts were compared to theoretical predictions. The model is based on an approximate solution of the diffusion equation for both aqueous and organic diffusion layers using a numerical scheme (finite difference in time and finite elements in space). The model may be evaluated on the basis of experimentally available parameters and gives time-dependent information previously inaccessible with a simpler steady-state diffusion model. For the cases studied, the model gave a very good correlation with experimental data, albeit with lower than expected diffusion coefficients for the organic phase. This model may address numerous open questions regarding the response time and memory effects of low-detection-limit ion-selective electrodes and for other membrane electrodes where ion fluxes are relevant.

The construction of a polymeric membrane ion-selective electrode traditionally required a relatively high concentration of the ion of interest in the inner filling solution (IFS); however, experimental evidence suggested that this has a deteriorating influence on the detection limit. For example, the low detection limit was greatly improved when complexing agents were present in the sample, indicating that the detection limit measured in the absence of such agents is not an intrinsic thermodynamic property of the ISE.[1,2] Large discrepancies between the detection limit of ISEs and their optical sensor counterparts were found.[3] Later, extremely large response differences of ISEs before and after initial contact with a solution containing the ion of interest provided the possibility of measuring unbiased, thermodynamic selectivity coefficients and initiated more intense research in this field.[4] Mathison et al. showed that an increased concentration of the primary ions in the inner solution leads to its extraction from the inner solution together with its counterions, forming ion fluxes from the membrane to the sample.[5] This process changes the ion activity at the phase boundary, thereby significantly worsening the detection limit. Understanding of these zero-current transmembrane processes has led to significant improvement of low detection limits of ISEs. Adequate buffering of the concentration of primary ions in the inner solution, thus keeping a low activity of the primary ions and a relatively high activity of the interfering ions, greatly improved the detection limit to nanomolar levels and lower.[6−11]

These advances have been accompanied by theoretical efforts to understand these processes and to predict the achievable detection limit. Initially a range of treatments considered fundamental coextraction and ion-exchange processes at both phase boundaries and steady-state fluxes to predict the concentrations of primary ions in the aqueous and organic diffusion layers.[12,13] Subsequently, a more simplified model was introduced that incorporated ion-exchange processes on the basis of current selectivity theory, thereby giving explicit equations that depended on directly experimentally available parameters.[8,9] It is today possible to predict the achievable detection limit and the optimal composition of the inner solution as well as the steady state response behavior of an ion-selective electrode with good accuracy if the membrane selectivity and sample composition are known. It was recently shown that this model is also applicable for the prediction of potential changes at the detection limit upon changing the thickness of the aqueous diffusion layer. This was applied to the development of an experimental method for the convenient

[†] Department of Chemistry.

[‡] Department of Mathematics.

(1) Morf, W. E.; Kahr, G.; Simon, W. *Anal. Chem.* **1974**, *46*, 1538.

(2) Morf, W. E. *The Principles of Ion-Selective Electrodes and of Membrane Transport*; Elsevier: New York, 1981.

(3) Bakker, E.; Willer, M.; Pretsch, E. *Anal. Chim. Acta* **1993**, *282*, 265.

(4) Bakker, E. *Anal. Chem.* **1997**, *69*, 1061.

(5) Mathison, S.; Bakker, E. *Anal. Chem.* **1998**, *70*, 303.

(6) Sokalski, T.; Ceresa, A.; Zwickl, T.; Pretsch, E. *J. Am. Chem. Soc.* **1997**, *119*, 11347.

(7) Malon, A.; Radu, A.; Qin, W.; Qin, Y.; Ceresa, A.; Maj-Zurawska, M.; Bakker, E.; Pretsch, E. *Anal. Chem.* **2003**, *75*, 3865.

(8) Ceresa, A.; Radu, A.; Peper, S.; Bakker, E.; Pretsch, E. *Anal. Chem.* **2002**, *74*, 4027.

(9) Ceresa, A.; Bakker, E.; Hattendorf, B.; Gunther, D.; Pretsch, E. *Anal. Chem.* **2001**, *73*, 343.

(10) Ion, A. C.; Bakker, E.; Pretsch, E. *Anal. Chim. Acta* **2001**, *440*, 71.

(11) Qin, W.; Zwickl, T.; Pretsch, E. *Anal. Chem.* **2000**, *72*, 3236.

(12) Sokalski, T.; Zwickl, T.; Bakker, E.; Pretsch, E. *Anal. Chem.* **1999**, *71*, 1204.

(13) Morf, W. E.; Badertscher, M.; Zwickl, T.; De Rooij, N. F.; Pretsch, E. *J. Phys. Chem. B* **1999**, *103*, 11346.

10.1021/ac049348t CCC: $27.50
Published on Web 09/14/2004

evaluation of the state of optimization of the inner solution.[14]

It is in the nature of any steady-state model that time-dependent phenomena are neglected, which makes it inadequate for the prediction of the real-time potential response, classified as short-, middle-, and long-term response changes. Short-term dynamics (milliseconds to several seconds) are normally controlled by the diffusion of ions from the sample bulk to the membrane surface and were thoroughly studied in the 1970s and 1980s by the integration of a first-order kinetic equation, such as ion dehydration, chemisorption, or a complex formation reaction,[15] on the basis of current−voltage−time curves of glass electrodes,[16] or by employing diffusion models based on the assumption that ion transport through the adhering laminar layer is rate-determining.[17,18] The influence of different parameters on the dynamic behavior of ion-selective electrodes was experimentally studied mostly with flow-jet systems.[19−21] Middle-term potential drifts[13] (minutes to hours) are especially important with ion-selective electrodes near the detection limit[9] or, for some membrane formulations, in the super-Nernstian response range[22] and are the principal focus of this paper. Long-term potential changes (many hours to days) primarily reflect slow changes in the bulk composition of the contacting aqueous phases, which are not considered here.

Two different approaches in explaining the mechanism that dictate the response function of ISEs have been topic of significant scientific debate. While advocates of the phase boundary potential model are using equilibrium parameters in the treatment of ISEs response function, treatment of ion transfer kinetics at the phase boundary and ion transfer across the membrane was used by researchers in favor of dynamic models. Recently, a review was published that describes advantages and disadvantages of both approaches.[23] Briefly, the most comprehensive dynamic model is based on the Nernst−Planck flux equation and provides results very similar to those obtained by the phase boundary potential model.[24] However, a serious practical drawback of the Nernst−Planck model is the experimental inaccessibility of numerous parameters, such as the individual mobilities of involved ions or the rate constants for the ion transfer through the phase boundary. The phase boundary potential model, by its nature, neglects migration processes in the membrane and the existence of a diffusion potential. It relies only on experimentally available data and, due to its predictive power, has been successfully applied in many works, by far outpacing the impact of dynamic models in the treatment of experimental data.

In this work, we are presenting a dynamic diffusion model that successfully explains both short and middle-term drifts and allows one to trace real-time potential response of an ion-selective electrode as well as to treat so-called memory effects. The model is based on a numerical method using finite difference discretization in time and finite element discretization in space. It gives an approximate solution of the diffusion equation in the aqueous and organic diffusion layers and treats the sample-membrane interface condition on the basis of current ion-exchange and ISE selectivity theory.

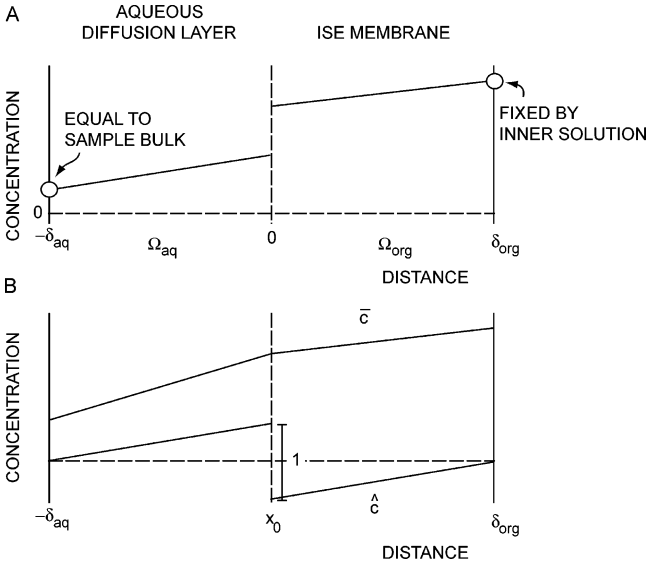

Figure 1. (A) Diffusion profiles in the membrane of thickness δ_{org} and Nernst diffusion layer in the contacting sample δ_{aq}, with the interface Γ at distance 0. The two boundary conditions for solving the diffusion equation are marked with circles. (B) The solutions $\bar{c}$ and $\hat{c}$, building blocks for obtaining the desired solution c (see text and Supporting Information).

THEORY

In this section, we describe the numerical method (finite element in space, finite difference in time; see refs 25 and 26 for an introduction to these methods) that we use to approximate a solution of the one-dimensional transmission problem with a nonlinear jump condition on an interface. This equation with these jump conditions has never before been treated in the mathematics literature.

Figure 1A shows two subdomains (here, these are two open intervals), $\Omega_{aq} = (-\delta_{aq}, 0)$ and $\Omega_{org} = (0, \delta_{org})$, and their union $\Omega = \Omega_{aq} \cup \Omega_{org}$ and a time interval $(0, T)$ (for some given $0 < T$). The boundary separating the two subdomains is $\Gamma = \{0\}$ − the interface. Given a function $c:\Omega \to \mathbb{R}$, we denote its restriction to each of the two subdomains by $c_\kappa = c|_{\Omega\kappa}$ for $\kappa =$ aq, or $\kappa =$ org.

The chemistry problem we are studying will be modeled by the following transmission problem: find a function $c(x, t)$ such that

$$c_{,t} - (Dc_{,x})_{,x} = 0 \quad \text{in} \quad \Omega \times (0, T) \tag{1}$$

(here, subscripts $_{,\xi}$ denote partial derivatives with respect to ξ) subject to the boundary conditions

(14) Radu, A.; Telting-Diaz, M.; Bakker, E. *Anal. Chem.* **2003**, *75*, 6922.
(15) Lindner, E.; Toth, K.; Pungor, E. *Anal. Chem.* **1976**, *48*, 1071.
(16) Buck, R. P. *J. Electroanal. Chem. Interfacial Electrochem.* **1968**, *18*, 363.
(17) Markovic, P. L.; Osburn, J. O. *AIChE J.* **1973**, *19*, 504.
(18) Morf, W. E.; Lindner, E.; Simon, W. *Anal. Chem.* **1975**, *47*, 1596.
(19) Lindner, E.; Toth, K.; Pungor, E.; Morf, W. E.; Simon, W. *Anal. Chem.* **1978**, *50*, 1627.
(20) Lindner, E.; Toth, K.; Pungor, E.; Berube, T. R.; Buck, R. P. *Anal. Chem.* **1987**, *59*, 2213.
(21) Huser, M.; Gehrig, P. M.; Morf, W. E.; Simon, W.; Lindner, E.; Jeney, J.; Toth, K.; Pungor, E. *Anal. Chem.* **1991**, *63*, 1380.
(22) Vigassy, T.; Ceresa, A.; Badertscher, M.; Morf, W. E.; Rooij, N. F. d.; Pretsch, E. *Sens. Actuators, B* **2001**, *76*, 476.
(23) Bakker, E.; Buhlmann, P.; Pretsch, E. *Talanta* **2004**, *63*, 3.
(24) Sokalski, T.; Lingenfelter, P.; Lewenstam, A. *J. Phys. Chem. B* **2003**, *107*, 2443.
(25) Johnson, C. *Numerical Solution of Partial Differential Equations by the Finite Element Method*; Cambridge University Press: Cambridge, 1987.
(26) Quarteroni, A.; Valli, A. *Numerical Approximation of Partial Differential Equations*; Springer-Verlag: Berlin, 1994.

$$c(-\delta_{aq}, t) = c_{aq,b}(t)$$

and

$$c(\delta_{org},t) = c_{org,b}(t) \quad \text{for } t \text{ in } (0, T) \tag{2}$$

Flux continuity across the interface (at the interface, $x = 0$) is represented by

$$D_{aq}c_{aq,x}(0, t) - D_{org}c_{org,x}(0, t) = 0 \quad \text{for } t \text{ in } (0, T) \tag{3}$$

In the above equations, $c_{aq,x}$ and $c_{org,x}$ are the gradients, or derivatives, of the primary ions in the aqueous diffusion layer and the concentration of the primary ion−ionophore complex in the membrane, respectively. The diffusion coefficient D is a given piecewise constant function

$$D(x) = \begin{cases} D_{org} \text{ for } x \in \Omega_{aq} \\ D_{org} \text{ for } x \in \Omega_{org} \end{cases} \tag{4}$$

The values of δ_{org} and δ_{aq} are the thicknesses of the membrane and aqueous diffusion layer, respectively. The boundary condition at the aqueous side assumes the constant concentration of the bulk solution, $c_{aq,b}$, at the position $-\delta_{aq}$. The assumption of a constant concentration of primary ion−ionophore complex at the inner side of the membrane, $c_{org,b}$ at δ_{org}, is a reasonable approximation with well-buffered inner solutions.[10] In certain cases, this boundary concentration can be accurately calculated from known membrane and inner solution compositions.[8,11,14]

The concentration relationship at the sample-membrane interface is the most uncommon feature in this treatment, and must be derived from the known ion-exchange equilibrium of such membranes. For analyte ions that partially exchange at this interface with interfering ions J of the same valency, the following simplified relationship may hold,

$$K_{I,J}^{pot} = \frac{c_{aq}(0, t)\{c_{Rorg} - c_{org}(0, t)\}}{c_{org}(0, t)c_{Jaq}} \tag{5}$$

where $K_{I,J}^{pot}$ is the experimentally accessible selectivity coefficient (which here is equal to an ion-exchange constant), and $c_{J,aq}$ and $c_{R,org}$ are the concentrations of interfering ion J in the aqueous phase and of the ion-exchanger in the organic phase, respectively. These two concentrations are high and therefore not expected to vary as a function of time and space in the indicated phase. Equation 5 is rewritten as

$$c_{aq}(0, t)c_{R,org} - K_{I,J}^{pot}c_{J,aq}c_{org}(0, t) = c_{aq}(0, t)c_{org}(0, t) \tag{6}$$

In simplified mathematical notation, the interface condition eq 6 is written as

$$\sigma_{aq}c_{aq}(0, t) - \sigma_{org}c_{org}(0, t) = \sigma_0 c_{aq}(0, t)c_{org}(0, t) \text{ for } t \text{ in } (0, T) \tag{7}$$

where σ_{aq}, σ_{org}, and σ_0 are given as nonnegative constants (the last constant is 1 for the physical situation discussed here).

To be precise $c_{aq}(0, t) = \lim_{\substack{x\to 0 \\ x<0}} c_{aq}(x, t)$ and $c_{org}(0, t) = \lim_{\substack{x\to 0, \\ 0<x}} c_{org}(x, t)$.

Finally, the relative potential was calculated on the basis of the phase boundary potential equation,

$$E = \frac{RT}{z_I F} \ln \frac{c_{aq}(0, t)}{c_{org}(0, t)} \tag{8}$$

where R, T, and F have their usual meaning (gas constant, temperature and Faraday's constant, respectively) and z_I is the charge of the primary ion.

Problems with jump condition (eq 7) have never been studied numerically or analytically in the mathematical literature. To discretize the partial differential equation using finite differences in time and finite elements in space the equation must be reformulated as a *weak problem*. This discretization (finite difference in time and finite elements in space) then yields a system of linear algebraic equations coupled to a single nonlinear constraint (quadratic equation, representing the nonlinear jump condition) which must be solved at each time step (that is, to advance the solution from time t to time $t + \Delta t$). Details of the *weak problem*, its discretization, and an efficient procedure for solving the linear system subject to the nonlinear constraint are given in the Supporting Information.

EXPERIMENTAL SECTION

Reagents. Silver ionophore IV(*O,O″*-bis[2-(methylthio)ethyl]-*tert*-butylcalix[4]arene, Ag IV), bis(2-ethylhexyl)sebacate (DOS), high molecular weight poly(vinyl chloride) (PVC), tetrahydrofuran (THF), potassium ionophore I (Valinomycin), 2-nitrophenyl octyl ether (NPOE), potassium chloride (KCl), potassium perchlorate ($KClO_4$), sodium chloride (NaCl), cation-exchanger resin (Dowex C-350 H^+ form, 30−80 mesh), and Silver Ion Standard solution (for ion-selective electrodes) were purchased from Fluka (Fluka Chemical Corp., Milwaukee, WI). Sodium tetrakis[3,5-bis(trifluoromethyl)phenyl]borate (NaTFPB) was purchased from Dojindo Laboratories (Japan). Lithium nitrate was from Fisher Scientific (Fair Lawn, NJ) in certified grade. Aqueous solutions were prepared by dissolving the appropriate salts in Nanopure purified water.

Membranes. The silver-selective membrane used for the fabrication of the electrodes contained 10.38 mmol kg^{-1} (0.83 wt %) Ag IV, 4.32 mmol kg^{-1} (0.45 wt %) NaTFPB, 32.00 wt % PVC, and 67.72 wt % DOS. The potassium-selective membrane contained 19.34 mmol kg^{-1} (2.15 wt %) Valinomycin, 5.04 mmol kg^{-1} (0.46 wt %) NaTFPB, 34.54 wt % PVC, and 62.85 wt % NPOE. The components (totaling 417 mg in the case of silver-selective membrane and 240 mg in the case of potassium-selective membrane) were dissolved in THF (5.0 mL or 2.0 mL) and poured into glass rings of i.d. 70 or 28 mm. Overnight evaporation yielded transparent membranes of ∼200-μm thicknesses. The thickness of the potassium-selective membrane (180 μm) was measured with a micrometer.

Electrodes. Three different types of electrodes were constructed. In a type A electrode, a tubing of 1/16 in. i.d.and 1/8 in. o.d. was inserted into the distal end of a tubing with 1/8 in. i.d. and 1/4 in. o.d. Type B electrodes consisted of a tubing with 1/8 in. i.d. and 1/4 in. o.d. Electrodes of types C were made from tubings of 1/4 in. i.d. and 3/8 in. o.d. Disks of 6-, 6-, and 9-mm diameter for the types A, B, and C, respectively, were punched from the corresponding membrane and glued to the plasticized

PVC tubings with a THF/PVC slurry. Silver-selective electrodes were conditioned for ~12 h in 10^{-3} M $LiNO_3$ using the conditioning solution as the inner solution. The selectivity coefficient for Ag^+ over Li^+ has been reported elsewhere as $\log K^{pot}_{Ag,Li} = -7.7$.[8] Potassium-selective electrodes were made as type B electrodes and were not conditioned prior the experiment. Two different inner solutions for these electrodes were made. The inner solution for electrode 1 contained 0.06 M of $KClO_4$ with the addition of 10^{-3} M KCl. The inner solution for electrode 2 was made according to electrode B from ref. 11 In this case, the inner solution was obtained by equilibration of 0.2 g of resin with 1 mL of 10^{-3} M KCl and contained 5.5×10^{-7} M K^+ and 1.1×10^{-3} M Na^+. The selectivity coefficient of potassium-selective membrane for K^+ over Na^+ has been reported as $\log K^{pot}_{K,Na} = -4.5 \pm 0.1$.[27]

EMF Measurements. All measurements with silver-selective electrodes were performed in a constant 10^{-5} M LiNO3 background while measurement with potassium-selective electrodes were conducted in 10^{-4} M NaCl. Electrodes were rotated at 1000 rpm using the rotator system described below. Potentials were measured with a 16-channel electrode monitor at room temperature (22 °C) in stirred solutions in the galvanic cell: Ag/AgCl/3M KCl/1M LiOAc/sample solution/ISE membrane/IFS/10^{-3} M NaCl/AgCl/Ag with a double-junction reference electrode (type 6.0729.100, Methrom AG, CH-9101 Herisau, Switzerland). The experiments were performed in a 100-mL polyethylene beaker pretreated overnight in 0.1 M HNO_3. All emf values were corrected for liquid-junction potentials according to the Henderson equation. Activity coefficients were calculated by the Debye−Huckel approximation.

Rotator System. A Pine Instrument Co. (Grove City, PA) analytical rotator (model ASR) and an ASR motor control box (1000 rpm/V, 100−10000 rpm range) were used for all experiments. Most necessary adjustments have been described elsewhere.[28] With the silver-selective electrodes, however, it was necessary to establish a salt bridge by slightly altering the described electrode construction. For type A and B electrodes, a 2-mm-long piece of tubing (1/16 in. i.d. and 1/8 in. o.d.) was inserted into the ion-selective membrane tubing ~5 mm from the distal end containing the membrane. For the wider type C electrodes, this same piece of tubing was first fitted into an intermediate tubing (2-mm long, 1/8 in. i.d., and 1/4 in. o.d.) before insertion into the membrane tube. After membrane attachment and conditioning, the electrode was assembled by inserting a plastic pipet tip filled with a cotton plug into the inner narrow tubing, and the top compartment was filled with 10^{-3} M NaCl as a bridge electrolyte. Potassium-selective electrodes did not require a salt bridge, and the inner solution was brought in direct contact with the Ag/AgCl electrode.

RESULTS AND DISCUSSION

The diffusion model described above is essentially based on the same assumptions as the steady-state treatments given earlier.[8] Briefly, solvent polymeric membrane electrodes with excess ionophore over lipophilic ion exchangers are used (the concentration of uncomplexed ionophore is always constant, and complexes are stable), the extraction process at the sample-membrane interface is described by thermodynamic means by utilizing membrane selectivity theory and assuming ion-exchange processes with interfering ions only,[8] and the concentrations at the inner membrane side are kept constant because a sufficiently strong ion concentration/ion buffer is assumed to be present in the inner solution. In contrast to previous work,[8] the treatment presented here is limited to primary and interfering ions of the same charge, such as well-established silver and potassium-selective ISEs. Further development of the model will include the possibility of treatment of primary and interfering ions of different charges. Both diffusion layers (aqueous and organic side of the interface) were divided into a fixed number of space elements, for which the model calculates the concentration of the primary ion (in the aqueous sample phase) or primary ion−ionophore complex (in the organic phase) throughout the preset time steps.

Short-Term Dynamics. The response time of ion selective electrodes has been a topic of intense scientific discussion and presents an interesting test bed for the diffusion model developed here. Several theories of transient potentials have been developed in the past by considering different approaches to the problem. The work of Shatkay summarizes those approaches.[29] As noted by Shatkay and confirmed in the later works, the model that most accurately describes the response time is obtained by assuming that ions have to diffuse through the stagnant layer to the phase boundary. Treatment of the model was first given by Markovic and Osburn[17] and Rangarajan[30] and lately described and compared with experiments by Morf[18] and Lindner.[15,19] At the time, two types of membranes were distinguished. Ion-exchange membranes were considered to have a constant composition, whereas for the neutral carrier membranes (considered in this work, as well), the free extraction of the primary ion and its counterions was assumed, enabling the establishment of electrolyte fluxes in the membrane. It is unfortunate that the effect of lipophilic ion-exchangers was not yet fully realized at the time, which did not allow researchers to develop membrane models as we know them today: carrier membranes of constant composition. The following are the equations used to describe the response time of ion-exchange type membranes:

$$E_t = E_\infty + S \log\left[1 - \left(1 - \frac{a_I^0}{a_I}\right) e^{(-t/\tau)}\right] \tag{9}$$

with

$$\tau = \frac{\delta^2}{2D_{aq}} \tag{10}$$

and of neutral carrier type membranes

$$E_t = E_\infty + S \log\left[1 - \left(1 - \frac{a_I^0}{a_I}\right) \frac{1}{1 + \sqrt{\frac{t}{\tau}}}\right] \tag{11}$$

with

$$\tau = \frac{D_{org} K^2 \delta^2}{{D_{aq}}^2} \tag{12}$$

where E_t is the electrode potential at time t after the sample activity

(27) Bakker, E. *J. Electrochem. Soc.* **1996**, *143*, L83.
(28) Ye, Q. S.; Meyerhoff, M. E. *Anal. Chem.* **2001**, *73*, 332.
(29) Shatkay, A. *Anal. Chem.* **1976**, *48*, 1039.
(30) Rangarajan, R.; Rechnitz, G. A. *Anal. Chem.* **1975**, *47*, 324.

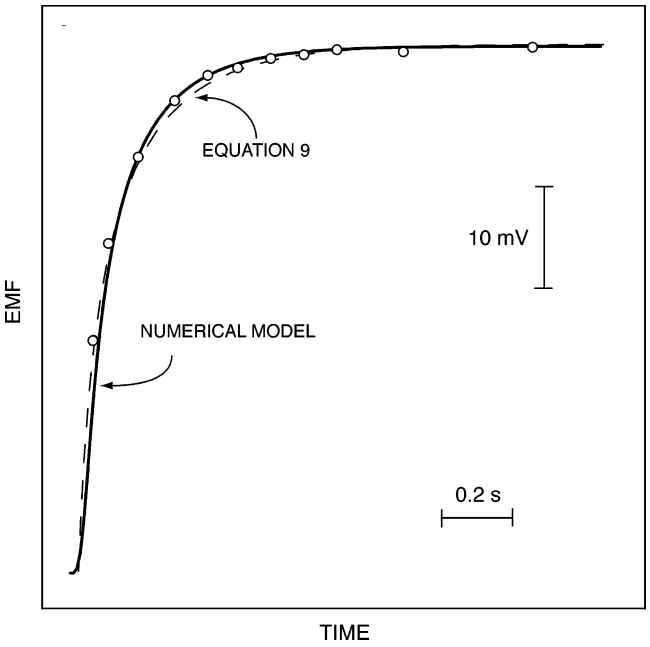

Figure 2. Prediction of the response time in the Nernstian response region for a sample activity change from 1 to 10 mM,[19] using eq 9 (dashed line), and the numerical model (solid line), demonstrating good correspondence. See text for other parameters used.

change; E_∞ is the final potential at sample activity a_I; S is the Nernstian slope of the electrode response; a_I^0 is activity of sample before the change; D_{org} and D_{aq} are the diffusion coefficients in the organic and aqueous phase, respectively; K is the electrolyte partition coefficient between the aqueous and the organic phase; and δ is the thickness of the aqueous layer. Today's membranes are carrier-based but with constant composition; hence, eq 9 was chosen for comparison with our model. Indeed, different values of D_{org} did not influence the response time with the model developed here.

Figure 2 shows a comparison of the response time obtained by eq 9 (dashed) and our model (solid line). For the modeling, the ion-exchange concentration was set as $R_T = 5$ mmol/kg (but variations were found to have no influence on the response time). The value of τ was obtained as 0.225 s from the work of Lindner on a potassium-selective electrode examined with a flow-jet system.[19] The aqueous diffusion coefficient for potassium, $D_{aq} = 1.96 \times 10^{-5}$ cm^2/s,[31] results in an aqueous diffusion layer thickness of 2.97×10^{-3} cm. The response time was found to be independent of $K_{I,J}^{pot} c_{J,aq}$ in the Nernstian response region of interest and arbitrarily set to 1×10^{-6}. As noted in the literature, a potassium activity change from 10^{-3} to 10^{-2} M with an electrode slope of 56.1 mV/dec was examined.[19] Time steps of 1 ms were used with our model, and each diffusion layer was divided into 50 space elements. Overall, both models give comparable results and provide some confidence of the applicability of the numeric diffusion treatment presented here. Note that the numerical model takes into account the diffusion time of ions through the aqueous diffusion layer, producing a visible lag in response time. Its zero time was therefore shifted to match the assumption of instant response described by eq 9 (see Figure 2).

Middle-Term Dynamics. The time response of ion-selective membranes measured near the detection limit or in a super-Nernstian response region cannot be appropriately modeled by eq 9 because slow changes in zero current transmembrane ion fluxes may lead to potential drift. In such cases, ion-exchange processes with interfering ions will generate a dynamically changing diffusion layer thickness in the organic phase. As established, the final potential is given by a steady state, not by an equilibration of the phase boundary with the bulk solution.[8] The numerical diffusion model developed above is most useful to describe such situations and was compared here with two different types of experiments involving highly silver-selective membranes as model systems. In the first situation, a membrane void of silver ions was exposed to alternating concentrations of silver, giving strongly drifting super-Nernstian responses that reflect the dynamic uptake of silver by the membrane (during which time lithium ions are expelled from the membrane). In the second type of experiment, the same membrane composition was used, but the silver activity in the sample was increased incrementally. In both of these scenarios, strong inward fluxes are observed that cannot be described in real time by the steady-state model.[8]

The first protocol explored here involved altering the concentration of the sample from 10^{-6} to 10^{-5} M of Ag^+, but not long enough to allow the establishment of the required equilibrium concentration of the silver ion on the organic side of the interface. Figure 3 shows the potential response for a silver electrode (type C) rotated at 1000 rpm (top plot) and the numerical model developed here (bottom). The numerical model gives a good correspondence with experimental data with $D_{org} = 1.1 \times 10^{-9}$ cm^2/s. Other parameters are the selectivity coefficient log, $K_{Ag,Li}^{pot} = -7.7$;[8] the activity of background ion log, $a_{Li} = -5.0$; the ion-exchange concentration in the membrane, $R_T = 4.3$ mmol kg^{-1}; the silver concentration at the inner membrane side, $c_{org,b} = 0$; $\delta_{org} = 200\ \mu$m; $\delta_{aq} = 46.6\ \mu$m (obtained from the rotational speed of the electrode); and $D_{aq} = 1.65\ 10^{-5}$ cm^2 s^{-1}. The diffusion coefficient in the membrane phase is an order of magnitude smaller than typically expected with membranes of this formulation.[32,33] Electrodes of type C had ~44% of exposed electrode area toward the inner solution, which deviates somewhat from a strictly one-dimensional diffusion geometry. To elucidate this, analogous experiments with electrodes with even smaller exposed surface areas were performed (type A, 6.3% and type B, 25%) and confirmed that such variations have an important influence on the response characteristics in the super-Nernstian region (data not shown). The diffusion coefficients needed to describe the experiments with type A and B electrodes were 4.8 and 7.8×10^{-10} cm^2 s^{-1}, respectively, even smaller than for type C. Effects of the concave membrane geometry might also partly explain the smaller than expected diffusion coefficients needed here.

Figure 4 shows the observed potential time response of a silver-selective electrode (type C) upon addition of incremental concentrations of silver in the sample (top plot) and the calculated response curves for the numerical model used here (bottom). The numerical model used the same parameters as for Figure 3, which gave acceptable agreement with experimental data. It should be pointed out that so far, there is no theoretical model that was

(31) Cussler, E. L. *Diffusion, mass transfer in fluid systems*; Cambridge University Press: Cambridge, 1984.

(32) Püntener, M.; Fibbioli, M.; Bakker, E.; Pretsch, E. *Electroanalysis* **2002**, *14*, 1329.

(33) Long, R.; Bakker, E. *Anal. Chim. Acta* **2004**, *511*, 91.

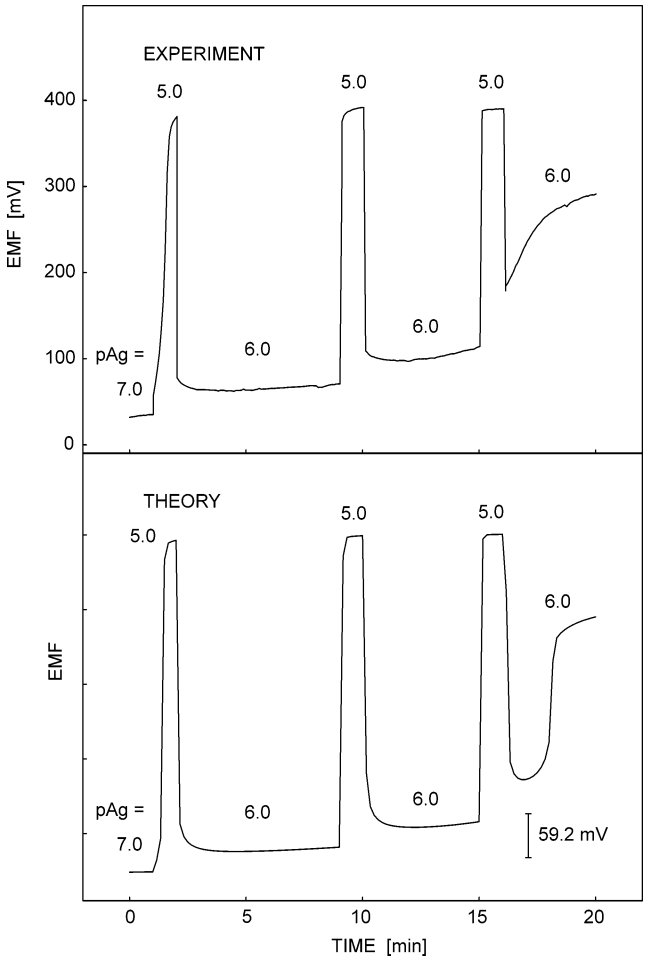

Figure 3. Experimental (top) and predicted (bottom) potential changes of a silver-selective membrane initially void of silver ions in response to alternating concentrations of silver nitrate (indicated as pAg values) in a background of 10^{-5} M $LiNO_3$. See text for other parameters used.

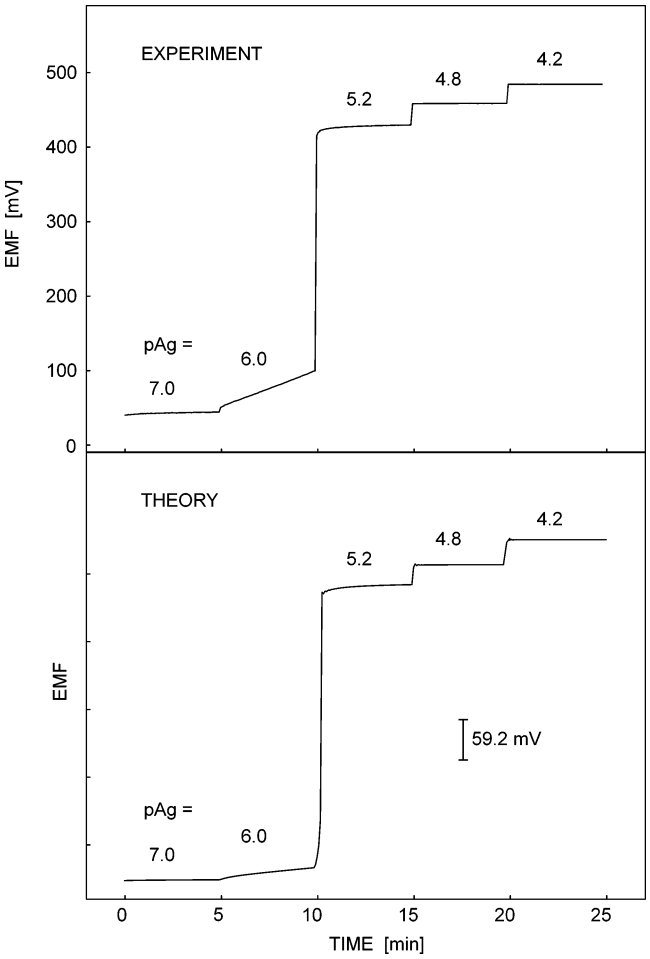

Figure 4. Experimental (top) and predicted (bottom) potential changes of a silver-selective membrane initially void of silver ions in response to incrementally increasing silver concentrations (indicated as pAg values) in a background of 10^{-5} M $LiNO_3$. All other parameters are identical to Figure 3.

successfully applied to the treatment of the potential drifts in the super-Nernstian response region. In light of the above observation that the exposed surface area of the membrane has an influence on response potential, it is reasonable to expect even better correlation in the cases approaching ideal one-dimensional diffusion theory.

The diffusion model was confirmed to agree with the earlier steady-state model at long times. Figure 5A shows the calculated response behavior of a cation-selective membrane, after reaching steady state in contact with a 10 nM sample, to a picomolar concentration step. The following parameters were used in the calculation: $R_T = 1.0$ mmol kg^{-1}; $Kc_J^{pot} = 10^{-13}$; $D_{org} = 10^{-8}$ cm^2 s^{-1}; $D_{aq} = 10^{-5}$ cm^2 s^{-1}; $\delta_{aq} = 100\ \mu$m; $\delta_{org} = 200\ \mu$m; concentration of primary ion at inner membrane side, $c_{org,b} = 1.0$ mmol kg^{-1}. This sample concentration is significantly lower than the steady-state detection limit of 0.3 nM,[8] indicated as a dotted horizontal line on the plot. As observed experimentally in the past, a significant potential drift is predicted, and the steady-state detection limit is not reached, even after 1 h of exposure in the dilute solution. As shown in the inset of Figure 5A, the reason for this sluggish behavior is the slow reconditioning time of the membrane. At the detection limit, a small level of ion exchange with interfering ions dictates the flux of ions in the direction of the sample, while in contact with a 10 nM solution, the transmembrane diffusion gradients are for this case negligibly small. Since it takes many hours for the membrane to recondition, the ion fluxes keep diminishing during this process, thus continuously lowering the local surface concentration of primary ions at the sample side.

Figure 5B confirms that the prolonged potential drift shown in Figure 5A is not an intrinsic property of ion-selective electrodes measured at low concentrations. A concentration step from 10^{-8} to 10^{-10} M is shown, with ion-selective electrodes of increasing selectivity (shown on the traces) toward the background interfering ion. As established earlier,[8] a 100-fold improved selectivity translates into a 10-fold-lower steady-state detection limit. All other parameters are as for Figure 5A. Clearly, the potential drifts are only significant for the membrane of poorest selectivity. If the sample concentration is significantly above the steady-state detection limit, the response is expected to be nearly instantaneous. This has important consequences to the design of ion-selective membranes for measurement at low concentrations and suggests that steady-state detection limits should be at least an order of magnitude lower than the targeted concentrations.

The steady-state model used in the past was incapable of predicting memory and hysteresis effects after exposure with elevated sample concentrations. Although the numerical model

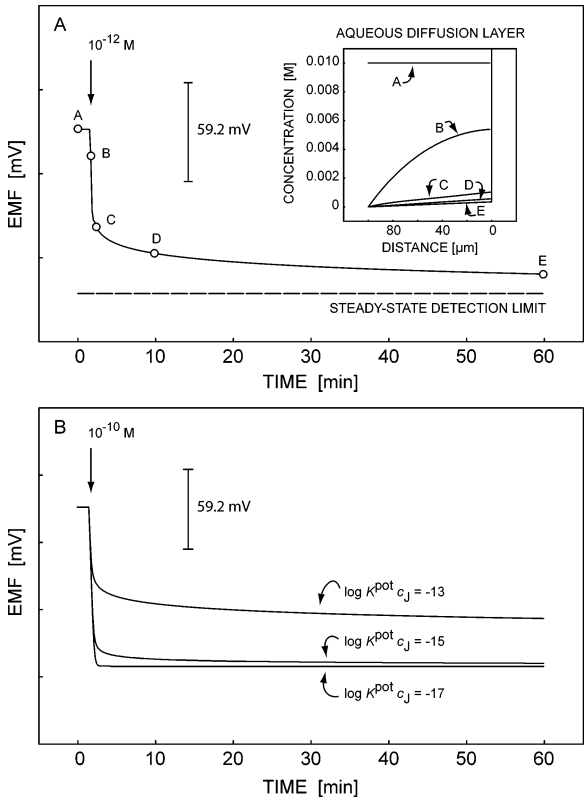

Figure 5. (A) Calculated potential−time response of an optimized silver-selective electrode in response to a 10^{-8}−10^{-12} M silver concentration change in the sample solution. The steady-state detection limit, 3×10^{-10} M, is indicated as a dashed horizontal line. The calculated concentration profiles on the sample side of the membrane are shown in the Figure for the indicated times. (B) Calculated potential−time response of three optimized silver-selective electrodes in response to a 10^{-8}−10^{-10} M silver concentration change in the sample solution. The three electrodes show the indicated variations in selectivity, with each 100-fold decrease in K^{pot} resulting in a 10-fold reduced steady-state detection limit. Response times are near-instantaneous for membranes of higher selectivity. See text for parameters used.

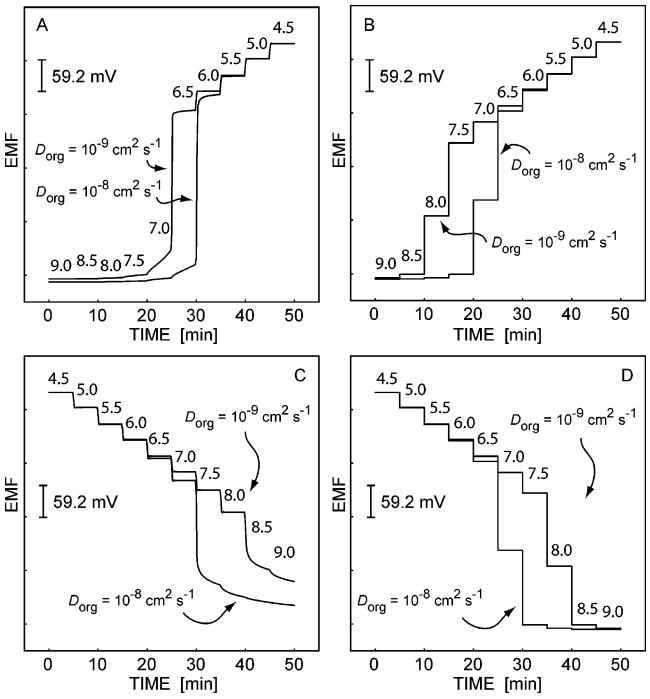

Figure 6. Calculated time responses for membranes showing a super-Nernstian response slope by exchanging 10% of primary ions with an interfering ion at the inner membrane side, thereby inducing an inward ion flux. (A) and)C) show the time response to increasing and decreasing ion concentrations, respectively. Sample concentrations are shown as picomolar values on the traces, which are calculated for two different diffusion coefficients in the membrane. (B) and (D) show the corresponding time traces calculated according to the established steady-state model.[8] All other parameters are as for Figure 5.

does not respect for coextraction processes at the sample side of the membrane, which may be relevant in contact with high concentrations, it gives valuable information upon exposure with moderately concentrated solutions. Figure 6A and C presents the calculated time responses of two different membrane electrodes upon exposure to incrementally increasing (Figure 6A) or decreasing sample concentrations (Figure 6C). The membranes were modeled to show an inward ion flux because of a 10% ion exchange at the inner membrane side with an interfering ion (in the model, $c_{org,b} = 0.9$ mmol kg^{-1}). Other parameters are as for Figure 5. The two traces shown are calculated for the two indicated membrane diffusion coefficients that vary 10-fold. Evidently, and as expected intuitively, the large potential change occurs at much higher sample concentrations when calibrating from low to high concentrations than from the high to low ones. Calibrations by sequential dilution are expected to show Nernstian response slopes down to lower concentration than expected on the basis of the steady-state model, shown in Figure 6B and D for the two experimental cases. Indeed, most early ion-selective membranes with demonstrated low detection limits were characterized by sequential dilution.[6,34,35] It is also evident that potentials in the super-Nernstian response region are not very stable and reproducible (see also Figure 3). Fortunately, instrumentally controlled ion-selective electrodes have recently been shown to alleviate this problem[36] so that super-Nernstian responses can now be utilized reliably for analytical purposes.[37] Note that the large super-Nernstian potential change predicted at steady-state occurs nearly an order of magnitude later for the case of increasing concentrations (Figure 6C), as compared to the results of the numerical diffusion model (Figure 6D). Decreased membrane diffusion coefficients lead to a shift of this potential jump to lower concentrations with any of the models, as established.[38,39]

Ion-selective membranes need to be properly conditioned before measurement; i.e., optimal transmembrane concentration gradients must be established to avoid undesired response behavior at low sample concentrations. Figure 7 shows potential drifts of two different potassium-selective electrodes during the process of conditioning. The inner solution of electrode 1 allows for strong electrolyte coextraction from the inner side, while it is

(34) Sokalski, T.; Ceresa, A.; Fibbioli, M.; Zwickl, T.; Bakker, E.; Pretsch, E. *Anal. Chem.* **1999**, *71*, 1210.
(35) Pergel, E.; Gyurcsanyi, R. E.; Toth, K.; Lindner, E. *Anal. Chem.* **2001**, *73*, 4249.
(36) Shvarev, A.; Bakker, E. *Anal. Chem.* **2003**, *75*, 4541.
(37) Shvarev, A.; Bakker, E. *J. Am. Chem. Soc.* **2003**, *125*, 11192.
(38) Ceresa, A.; Sokalski, T.; Pretsch, E. *J. Electroanal. Chem.* **2001**, *501*, 70.
(39) Fu, B.; Bakker, E.; Yun, J. H.; Yang, V. C.; Meyerhoff, M. E. *Anal. Chem.* **1994**, *66*, 2250.

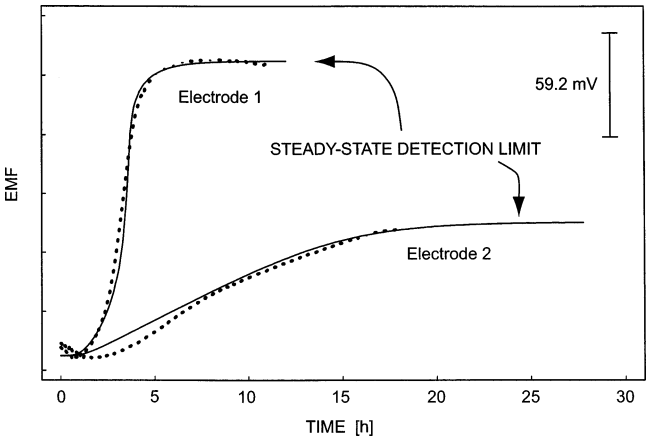

Figure 7. Conditioning times of two potassium-selective membranes with potassium exposure only from the inner side. Solid lines: theory. Dotted lines: experimental data. Electrode 1: strong electrolyte coextraction from the inner side is allowed ($x = 2.81$ where $x = c_{org,b}/R_T$, see text for calculation parameters). Electrode 2: well-buffered inner solution with $x = 1.00$.

well-buffered in the case of electrode 2 (for compositions see the Experimental Section). The electrodes were assembled, and the potentials were recorded starting at time zero. The full lines represent the calculated potentials, whereas the dotted lines show the experimental data. The potential in both cases starts at a low value, dictated by the response to the interfering sodium ions which are present at a concentration of 10^{-4} M. Gradually, they are replaced by potassium ions from the backside of the membrane, and the potential increases, approaching the steady-state values. Interestingly, this conditioning time is very different for the two examined cases. The steady-state limit is reached after ~5 h for electrode 1, but electrode 2 requires ~20 h for the same process. This drastic difference may be understood by the origin of the magnitude of the transmembrane ion flux. For electrode 1, the steady-state concentration gradient across the membrane is mainly dictated by the level of coextraction at the inner membrane side. Once potassium ions start to fill up the sample side of the membrane, the steady-state gradient starts to become dictated mainly by the potassium concentration at the inner side (that concentration is more than twice the concentration at the sample side). For electrode 2, the steady-state gradient is much more shallow and, hence, takes a longer time to fully establish. A good agreement between theory and experiment was achieved by using only experimentally available data. The parameters used in these calculations were as follows: $D_{aq} = 1.96\ 10^{-5}$ cm^2 s^{-1}, log $K^{pot}_{K,Na} = -4.6$ (within the experimental error of ref 27), $D_{org} = 7 \times 10^{-9}$ cm^2/s, the activity of background ion log $a_{Na} = -4.0$, the ion-exchange concentration in the membrane $R_T = 5.04$ mmol kg^{-1}, $\delta_{org} = 180$ μm, and $\delta_{aq} = 46.6$ μm (obtained from the rotational speed of the electrode). Note the diffusion coefficient used in the calculation is 30% smaller than the traditionally accepted value.[32,33] The calculation of $c_{org,b}$ was performed according to eq 16 from the reference.[14] The coextraction constant, log $K_{coex} = 28\ 380 \pm 530$, was calculated from the experimental data given by Qin et al.[40] For electrode 1, $c_{org,b} = 14.2$ mmol kg^{-1} was calculated and used in the model. From the composition of the inner solution of electrode 2 (see the Experimental Section), $c_{org,b} = 4.78$ mmol kg^{-1} was calculated, but because of the absence of a super-Nernstian response slope,[11] a concentration matching that of the ion-exchanger was chosen ($c_{org,b} = 5.04$ mmol kg^{-1}). Moreover, using the steady-state model for predicting the lower detection limit of this system based on this latter value of $c_{org,b}$[8] shows a very good correspondence with the experimentally obtained data in the same work.

Calculations were also performed for the silver-selective system described in this work (not shown) with the same parameters as for potassium, except silver's own diffusion coefficient in water, R_T, and $K^{pot}_{Ag,Na}$ (see above). This system, with a better membrane selectivity, showed even slower conditioning times. A well-buffered inner solution giving $c_{org,b} = 4.32$ mmol kg^{-1} showed a 40-h conditioning time. These calculations establish that it takes a much longer time to condition membranes for use at low concentrations than traditional nonoptimized ISE membranes. Prolonged exposure at both membrane sides,[34] predoping of the membrane with a salt of the primary ion,[9] or sequential conditioning with solutions of decreasing concentrations[41] have therefore all been reported in the literature for a good reason.

CONCLUSIONS

Understanding zero-current transmembrane diffusion processes is of paramount importance to the characterization and optimization of ion-selective electrodes with low detection limits or in cases in which nonequilibrium processes are relevant, such as with super-Nernstian response slopes. So far, steady-state diffusion models provided explicit analytical solutions that remain highly valuable for optimization and planning purposes. Here, a model based on numerical finite element analysis gives time-dependent information of the concentration profiles in the organic and aqueous phases. It was applied to membranes initially void of primary ions as a challenging model system. The smaller than expected membrane diffusion coefficients required to give good predictions were partly needed because practical membrane electrodes do not appear to perfectly obey one-dimensional diffusion theory. Still, the numerical model was able to trace the experimental potential transients very well. This makes it now possible to adequately predict time-dependent response behavior, memory effects, potential drifts, and anticipated conditioning times of such important potentiometric sensors.

ACKNOWLEDGMENT

The authors thank the National Institutes of Health (Grant E.B.002189) for financial support of this research.

SUPPORTING INFORMATION AVAILABLE

Further details on numerical modeling. This material is available free of charge via the Internet at http://www.pubs.acs.org.

Received for review May 3, 2004. Accepted August 4, 2004.

AC049348T

(40) Qin, Y.; Bakker, E. *Anal. Chem.* **2002**, *74*, 3134.

(41) Vigassy, T.; Gyurcsanyi, R. E.; Pretsch, E. *Electroanalysis* **2003**, *15*, 1270.